European Water 85/86: 25-35, 2024.
© 2024 *E.W. Publications*

Characterization of 1-hr maximum rainfall values in Calabria, southern Italy, by means of the ERA-5 reanalysis

Francesco Chiaravalloti, Roberto Coscarelli* and Tommaso Caloiero

Research Institute for Geo-Hydrological Protection, National Research Council of Italy, Rende (CS), Italy
** e-mail: roberto.coscarelli@cnr.it*

Abstract: Heavy precipitation events are likely to become more frequent in most parts of Europe; yet, records of hourly precipitation are often insufficient to study trends and changes in heavy rainfall. Atmospheric reanalyses are an important source of long-term meteorological data, often considered as a solution to overcome the unavailability of direct measurements. Among the available reanalyses, the fifth generation of the ECMWF Atmospheric Reanalysis (ERA5) dataset, released by the European Centre for Medium-Range Weather Forecasts (ECMWF), can be considered one of the state-of-the-art products. In this paper, data from the ERA5-land reanalysis dataset were first used to detect possible trends in the 1-hr maximum rainfall values in a region of southern Italy and then the monthly distribution of these values has been analysed. To check the rainfall trend, the widely recognized non-parametric Mann–Kendall test and the Theil–Sen slope estimator have been employed at monthly, seasonal and annual scales considering a significant level equal to 95%. Then, the time frame 1961-2020 was divided into three intervals, and for each one, considering the entire study area, the frequency distribution of the months recording the annual maxima was calculated. Results showed a positive tendency of the maximum 1-hr rainfall on a yearly scale. This tendency is not uniform for all the seasons: positive in spring, summer and autumn, negative for winter but with a few number of cells involved. These not-uniform tendencies are also confirmed on a monthly scale. Finally, as regards the temporal distribution of the occurrence of the yearly maximum 1-hr rainfall, initially the maximum values mostly occurred in October while, in the more recent sub-period, September is the month with the highest number of occurrences of these values.

Key words: Rainfall; ERA5; trend; Calabria.

1. INTRODUCTION

One of the most significant inputs and fundamental problems for hydrological science and practices is the rainfall patterns (Ahammed et al. 2014), commonly needed for flood forecasts, hydrological modeling, drainage structure construction, water resource availability, etc. (e.g., Lagouvardos et al. 2013; Petroselli et al. 2022). The number of observations in hydro-meteorological networks has been steadily declining in recent years due to high maintenance costs and the requirement for skilled personnel (Turnipseed & Sauer 2010). Thus, this problem becomes more and more crucial and it often causes uncertainties in the hydrologic and hydraulic model applications or in the estimations of meteorological parameters (Sabzevari 2017). As an example, the temporal distribution, frequency, and duration of rainfall are required to accurately predict the runoff in catchments by means of hydrological and hydrodynamic models, whose input parameter values are very sensitive to the rainfall changes (e.g., Walega et al. 2016, Petroselli et al. 2020). The design rainfall is often evaluated using statistical techniques based on theoretical distribution functions when enough long-observed rainfall data are available. Another method is to recreate the sequences of rainfall characteristics using radar observations that also consider the geographical variability of the rainfall field (Wright et al. 2013). It is frequently necessary to employ the more generally accessible satellite-based products because radar meteorological data are not readily available in certain parts of the world (Siddique-E-Akbor et al. 2014). When compared to gauge-based data, the satellite and radar outputs typically underestimate extreme rainfall (e.g., Bharti et al. 2016; Chen et al. 2020), given also the different spatial resolutions. Radar and satellite precipitation products represent an estimate of areal values averaged over a certain pixel, while raingauge data

are the real measurements of rainfall at a site.

Another source of data comes from the meteorological reanalysis that refers to the process of reconstructing a comprehensive representation of past weather conditions using a combination of observational data, such as surface observation, radiosonde measurements and satellite data, with advanced numerical weather prediction models. The assimilation process adjusts the model output to match the available observations, resulting in a high-quality dataset with consistent and detailed spatial and temporal resolution over large geographic regions, that represent the best estimate of historical weather conditions. Reanalysis datasets find widespread use across various fields of scientific research, including meteorology, climate science, hydrology and environmental science. For example, reanalysis datasets are widely used to study climate variability and the impacts of climate change (Xu et al. 2021; Monteiro and Morin 2023; Hanna et al 2022), analyze extreme weather events (Hu and Franzke 2020; Bezak and Mikoš 2020; Reder et al. 2022), monitoring drought conditions (Almendra-Martín et al. 2021; Vicente-Serrano et al. 2023; Palazzolo et al. 2023) and for hydrological modelling (Tarek et al. 2020; Longo-Minnolo et al. 2022; Essou et al. 2017), just to mention a few possibilities.

Numerous researches have examined precipitation trends and variability, and they have produced data showing either an increase or decrease in the frequency and intensity of heavy rainfall events worldwide aiming various aspects (designing of hydraulic structures, flood control measures, etc.). Mann-Kendall test is the method most researchers have used to identify these trends (e.g., Tabari & Talaee 2011; Caloiero et al. 2019). Other researchers (e.g., Kuo et al., 2011; Sirangelo et al. 2015; Caloiero et al. 2020) have used other methodologies, such as the dynamic factor analysis, a stochastic approach, the Innovative Trend Analysis, and so on.

In this paper, rainfall data from 1950 to 2020 from the ERA5-land reanalysis dataset were first used to detect possible trends in the 1-hr maximum yearly rainfall values in Calabria (southern Italy), analysing also the monthly distribution of these values. To detect the rainfall trend, the Mann–Kendall test and the Theil–Sen slope estimator have been employed at various scales, considering a significant level equal to 95%. Then, dividing the period 1961-2020 into three intervals, the months recording the annual maxima were evidenced for each sub-period aiming to the investigation of eventual changes of the occurrences of these maxima within the year.

2. CASE STUDY AND DATA

2.1 The Calabria region

The study area encompasses the Calabria region, situated in southern Italy, which is characterized by its distinctive geographic and climatic features. Spanning approximately 15,080 km² with a coastline of 738 km along the Ionian and Tyrrhenian Seas, Calabria presents an oblong shape, stretching 248 km in length and varying in width from 31 to 111 km. Bordering the Basilicata region to the north for 80 km, Calabria showcases a diverse terrain, comprising 42% mountainous, 49% hilly, and 9% flat areas. While not boasting towering peaks, it remains one of Italian most mountainous regions, with heights reaching up to 2,267 m above sea level (m a.s.l.) and an average elevation of 597 m a.s.l. (Figure 1).

The region's climate exhibits significant variability, characterized by a Mediterranean climate with dry, subtropical summers. During summer, the Azores anticyclone dominates, promoting dry and temperate conditions, while coastal and inland breezes prevail. Conversely, in winter, fall, and spring, the retreat of the Azores anticyclone and the extension of the Siberian high over Northern Europe and Scandinavia usher in Mediterranean cyclones, resulting in colder and more humid conditions.

The complex topography of Calabria profoundly influences its precipitation patterns (Coscarelli and Caloiero 2012). Orographic effects, highlighted by Colacino et al. (1997), generate distinct rainfall gradients between the Tyrrhenian and Ionian sides of the peninsula. The Ionian side,

influenced by African currents, experiences short yet intense precipitation events, while the Tyrrhenian side benefits from milder temperatures and substantial orographic precipitation due to western air currents.

Inland areas exhibit colder winters, often accompanied by snow, and cooler summers with sporadic precipitation, in contrast to the milder coastal zones.

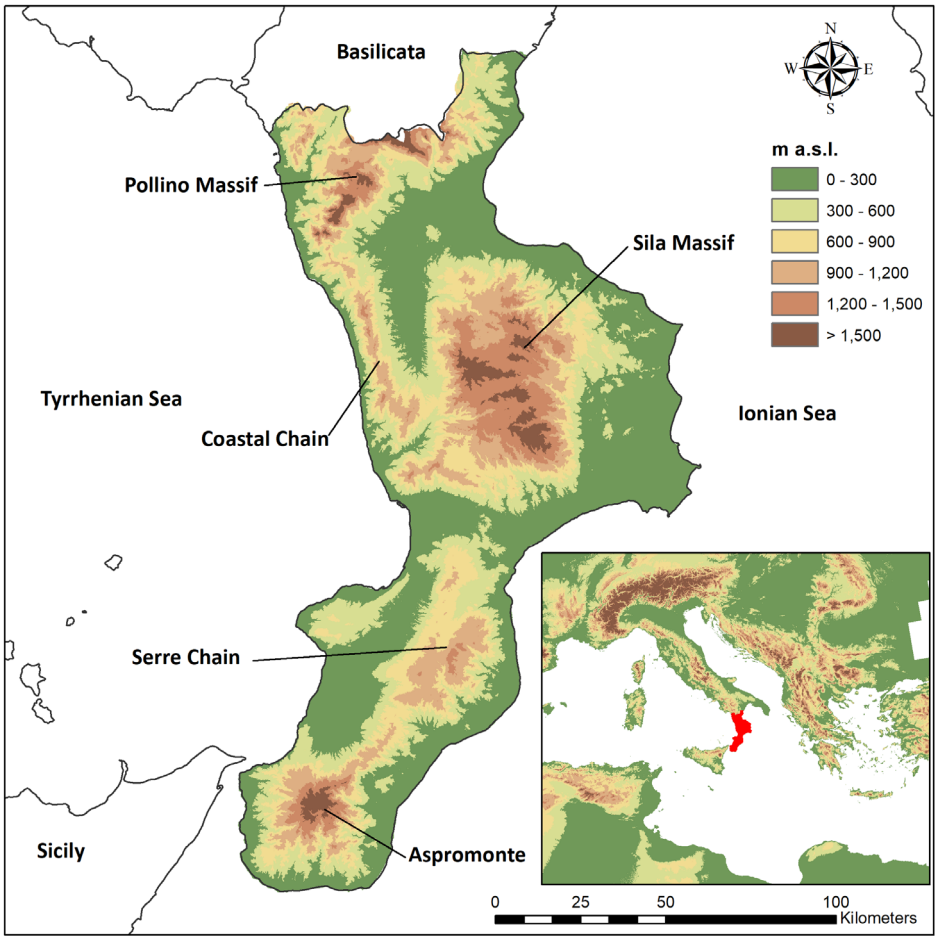

Figure 1. The study area (Calabria – southern Italy).

2.2 The ERA5-Land Reanalysis

ERA5-Land is the land component of the global reanalysis ERA5 developed by the European Centre for Medium-Range Weather Forecasts (ECMWF). It is based on advanced data assimilation techniques, including 4D-Var and Ensemble Kalman Filter (EnKF), to effectively integrate observational data into the model and reduce uncertainties in the reanalysis output (Muñoz-Sabater et al. 2021).

ECMWF has a long-standing involvement in atmospheric reanalysis, with ERA5 being the fifth generation in its reanalysis series. The organization began reanalysis efforts in 1979 with the FGGE project, followed by ERA-15 in the mid-1990s, ERA-40 between 2001 and 2003, and ERA-Interim, which was produced from 2006 to 2019. Each new reanalysis typically features higher horizontal resolution, more advanced data assimilation techniques, and improvements in forecast model development. All reanalyses include a land component, and starting with ERA-40, ocean surface wave data and atmospheric ozone products have also been incorporated (Hersbach et al. 2020).

Compared to its predecessors, ERA5-Land incorporates Earth's surface processes more accurately, providing a state-of-the comprehensive description of the land surface variables, including precipitation, soil moisture and temperature, with a spatial resolution of 9 km (0.1 x 0.1) and a temporal resolution of 1 hour. Data are available from 1950 up to almost the present and the

high resolution allows for detailed analysis of weather and climate phenomena even on a regional scale. The dataset is freely available to the scientific community and can be accessed through the ECMWF Climate Data Store (Muñoz Sabater 2019). In addition, ERA5-Land is constantly updated and improved, ensuring that users have access to the most up-to-date information on land surface variables.

In this work, the total precipitation field of the ERA5-Land reanalysis dataset (Figure 2), downloaded from the Copernicus Climate Change Service (C3S), was used for each of the 141 cells (dimension 9x9 km^2) in the Calabria region to derive the time series of hourly precipitation amount from 1950 until 2020. This parameter represents the accumulated liquid and frozen water, comprising rain and snow, falling to the Earth's surface, and it includes both large-scale and convective precipitation. The sequence of months in which the annual maximum of hourly rainfall occurs was then calculated for each cell, obtaining a succession of 71 values for each of them.

3. METHODOLOGY

To detect existing trends, in this paper two non-parametric tests have been used: the Theil–Sen estimator (Sen 1968) for the evaluation of the slopes of the trends and the Mann–Kendall test for the assessment of the statistical significance (Mann 1945; Kendall 1975).

About the Mann–Kendall test, given n data at times j and k ($j > k$), the statistic S is given by:

$$S = \sum_{k=1}^{n-1} \sum_{j=k+1}^{n} sgn\left(x_j - x_k\right) \tag{1}$$

in which the sign function can be equal to 1 (if $x_j > x_k$), 0 (if $x_j = x_k$) or -1 (if $x_j < x_k$).

Given the S values and the variance of S, the Mann–Kendall test statistic can be then evaluated as follows:

$$Z_{MK} = \begin{cases} \dfrac{S-1}{\sqrt{Var(S)}} & for\ S > 0 \\ 0 & for\ S = 0 \\ \dfrac{S+1}{\sqrt{Var(S)}} & for\ S < 0 \end{cases} \tag{2}$$

With respect to the Theil–Sen estimator, given $x_1, x_2, \ldots, x_n$ rainfall observations at times $t_1, t_2, \ldots, t_n$ (with $t_1 \leq t_2 \leq \ldots \leq t_n$), for each N pairs of observations x_j and x_i taken at times t_j and t_i, the gradient Q_k can be calculated as:

$$Q_k = \frac{x_j - x_i}{t_j - t_i} \qquad for \quad k = 1, \ldots, N \tag{3}$$

with $1 \leq i \leq j \leq n$ and $t_j > t_i$.

The estimate of trends in the data series $x_1, x_2, \ldots, x_n$ can then be calculated as the median Q_{med} of the N values of Q_k, ranked from the smallest to the largest:

$$Q_{med} = \begin{cases} Q_{[(N+1)/2]} & if\ N\ is\ odd \\ \dfrac{Q_{[N/2]} + Q_{[(N+2)/2]}}{2} & if\ N\ is\ even \end{cases} \tag{4}$$

The Q_{med} sign reveals the trend behaviour, while its value indicates the magnitude of the trend.

4. RESULTS

The results of the trend analysis applied to the annual, monthly and seasonal maximum 1-hr rainfall values are presented in Figures 2-6. In particular, Figure 2 shows the percentages of grid points with a positive or negative trend for the different timescales.

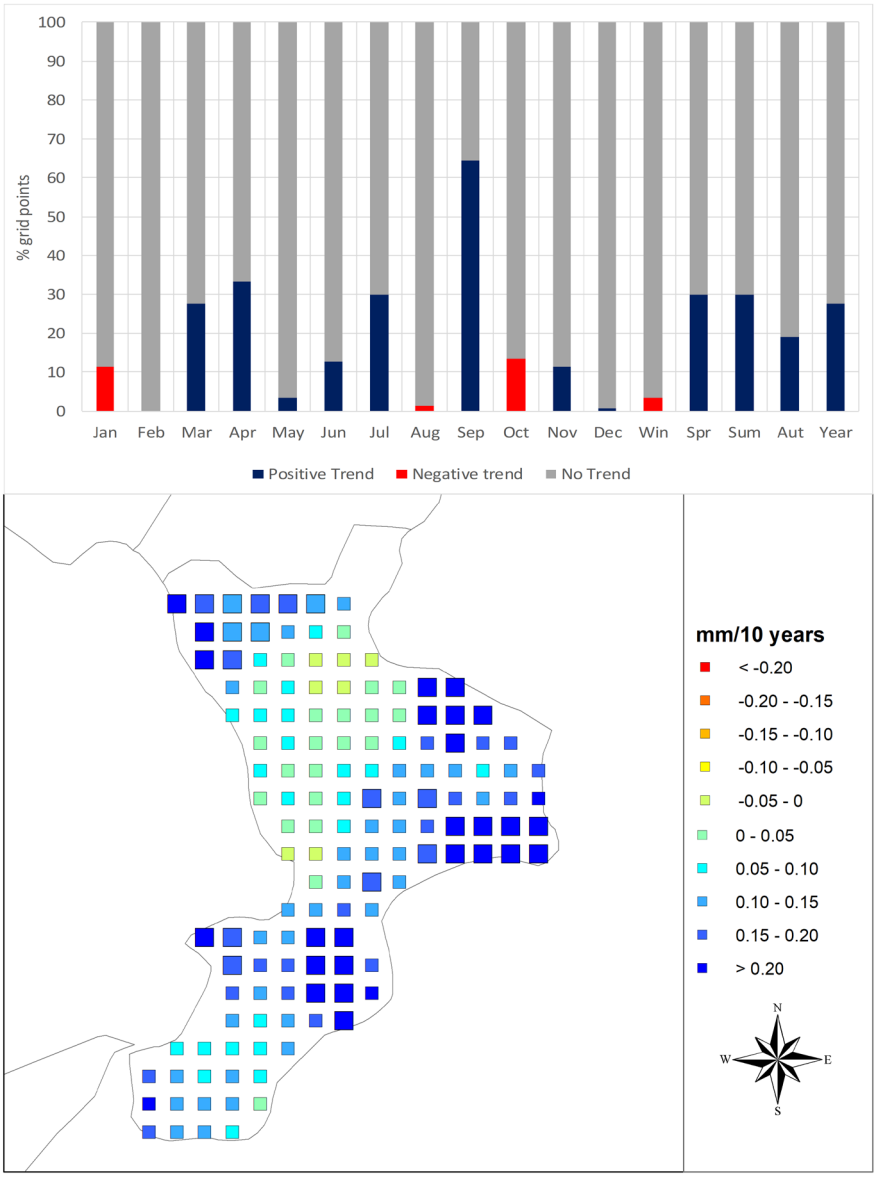

Figure 2. Percentages of grid points with a positive or negative trend for the different timescales (up) and the spatial distribution (down) of the results for the annual scale obtained by means of the Theil–Sen estimator .

As a result, at annual scale, a positive trend was detected. In fact, about 28% of the grid points showed a positive trend, while significant negative trends have not been identified. The positive trend of the yearly maximum 1-hr rainfall values is spatially distributed throughout the entire study area, with the highest increment detected in the eastern side of the region, where the application of the Theil-Sen estimator has allowed us to identify an increase of more than 0.2 mm/10 years (Figure 2). It is worth noting that, in Figure 2, as well as in the following figures explaining the spatial distribution of the trends, squares dimension indicates the significance level (SL) of the trend. In particular, large dimension squares suggest a significant trend (SL = 95%), while small squares

otherwise, i.e., a not significant trend.

At seasonal scale, in winter only 3.5% of the grid points showed a significant trend of the maximum 1-hr rainfall and with a negative sign (Figure 2). These negative trends, with a maximum magnitude between -0.10 and -0.15 mm/10 years, are localized in the northern side of the region, in the area of the Pollino Massif, one of the main mountains of the region (Figure 3). As regards the trend of the maximum 1-hr rainfall in the winter months (i.e., December, January and February) only in January relevant results have been obtained, with more than 11% of the grid points showing a negative trend (Figure 2). On the contrary, in December and in February mainly not significant results have been obtained (Figure 2). From a spatial point of view, the negative tendencies detected in January, reaching a maximum decrease between -0.15 and -0.2 mm/10 years, mainly involve the eastern sector of the region in the area between the southern part of the Sila Massif and the Ionian Sea (Figure 3).

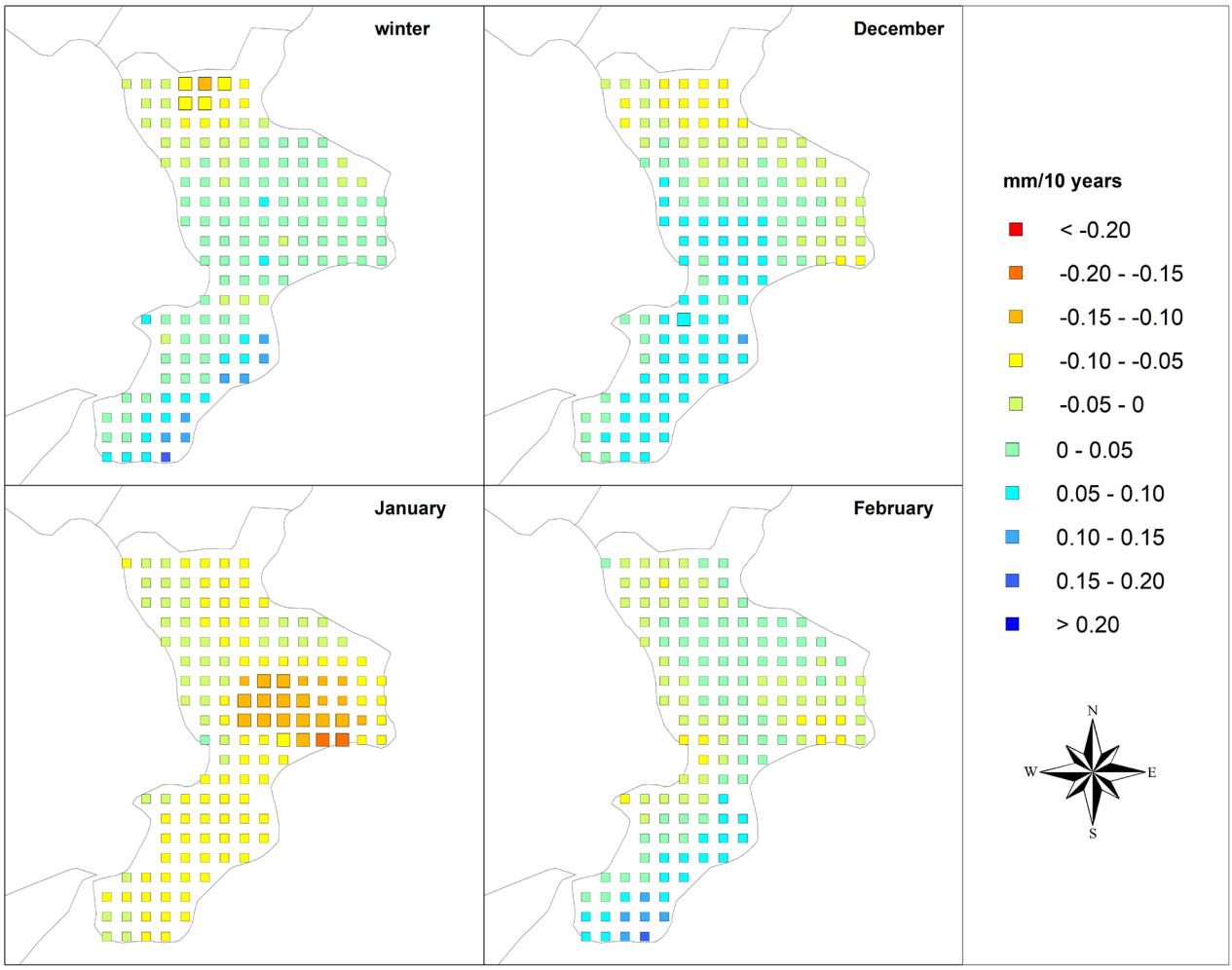

Figure 3. Spatial distribution of the trend results for winter obtained by means of the Theil–Sen estimator.

Differently from winter, in spring about 30% of the grid points showed a significant positive trend of the maximum 1-hr rainfall and no negative trends have been detected (Figure 2). These grid points showed a maximum increase of more than 0.2 mm/10 years and are localized in all the southern part of the region, from the Tyrrhenian Sea to the Ionian Sea (Figure 4). On a monthly scale, 27.7%, 33.3% and 3.5% of the grid point showed significant (positive) trend values in March, April and May, respectively (Figure 2).

Similar to the spatial distribution of the trend in the spring season, in March the grid points showing significant trend (maximum increase > 0.2 mm/10 years) have been detected in the southern part of the region (Figure 4). On the contrary, in April (maximum increase between 0.15

and 0.2 mm/10 years) and May (maximum increase between 0.10 and 0.15 mm/10 years) the positive trends mainly involve the central and northern areas and the northeastern area of the region, respectively (Figure 4).

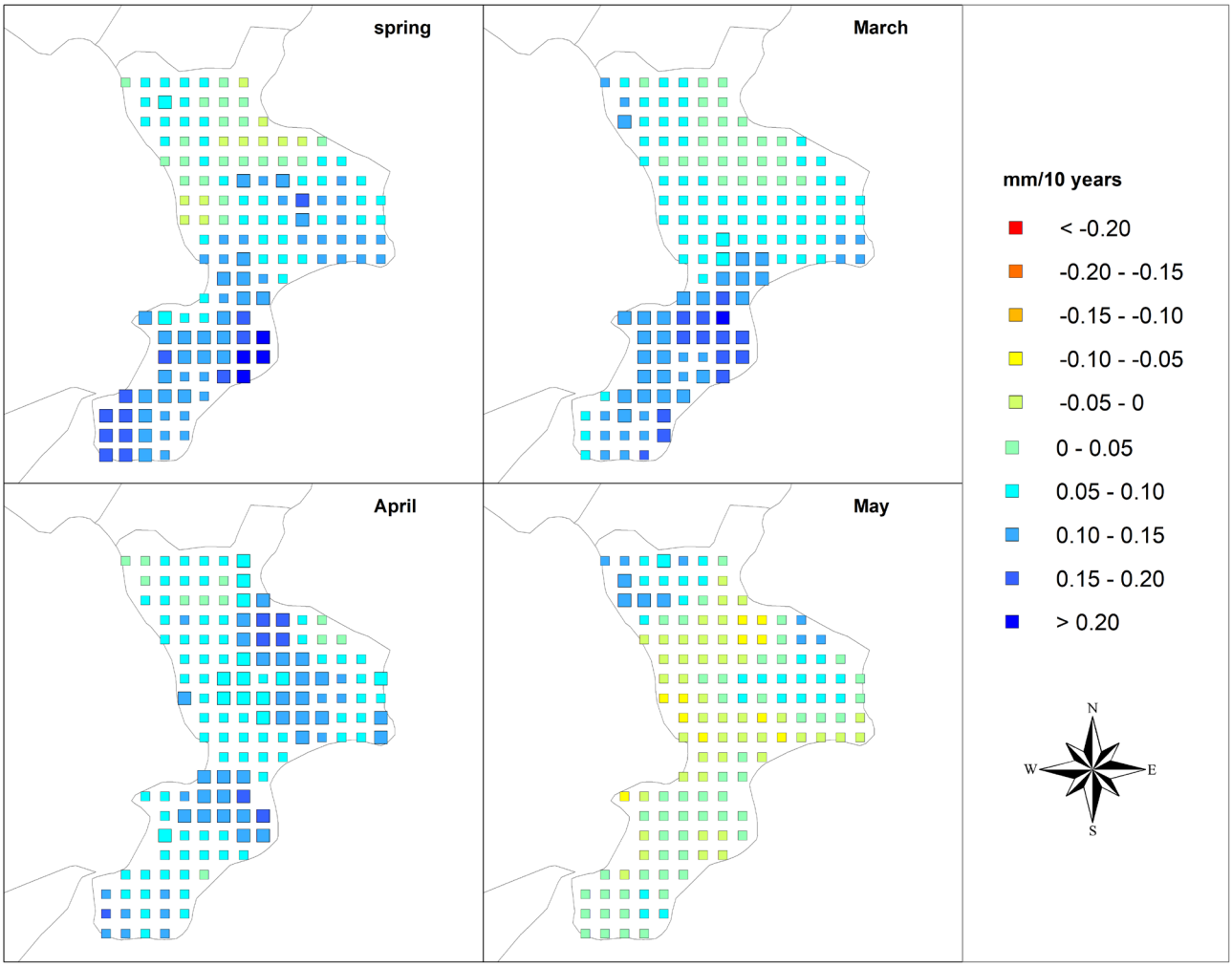

Figure 4. Spatial distribution of the trend results for spring obtained by means of the Theil–Sen estimator.

Results of the trend analysis performed in the summer season is quite similar to the one obtained in spring, in both percentages of significant positive trend and spatial distribution of the grid points showing significant results. In fact, also in summer 29.8% of the grid points, localized in the southern part of the region, evidenced a significant positive trend of the maximum 1-hr rainfall (with no negative trends), and showed a maximum increase of more than 0.2 mm/10 years (Figures 2 and 5). A similar trend behavior has been identified in June (12.8% of the grid points) and July (29.8% of the grid points) but with a different spatial distribution of the results (Figure 2). In fact, while in June significant positive trends have been detected in the southern part of the region, in the area of the Aspromonte Massif, in July the northern part of the region, from the Sila Massif to the Pollino Massif, is characterized by grid points showing a positive trend with a magnitude higher than 20 mm/10 years. Differently from June and July, in August only negative significant trends (1.4% of the grid points) have been identified (Figure 2), with a maximum decrease between -0.15 and -0.2 mm/10 years (Figure 5).

Finally, in autumn, slightly more than 19% of the grid points showed a significant positive trend of the maximum 1-hr rainfall without any negative trend (Figure 2). These trends are localized in the north-eastern side of the region, in the area of the Pollino Massif, and in the central part of the region, in the hilly area between the Sila Massif and the Ionian Sea (Figure 6), with increasing

values higher than 0.2 mm/10 years. On a monthly scale, remarkable values have been evaluated in September, with about 65% of the grid points showing significant positive values, while in October and November only 13.5% and 11.3% of the grid points showed significant results, respectively, negative for the first and positive for the latter (Figure 2). Given the high percentage of positive tendencies detected in September (reaching a maximum increase higher than 0.2 mm/10 years), these values are distributed across the entire region, without any particular spatial behavior (Figure 6). On the contrary, in October and November the significant trends mainly involve the central part of the region with magnitude lower than -0.2 mm/10 years and higher than 0.2 mm/10 years, respectively (Figure 6).

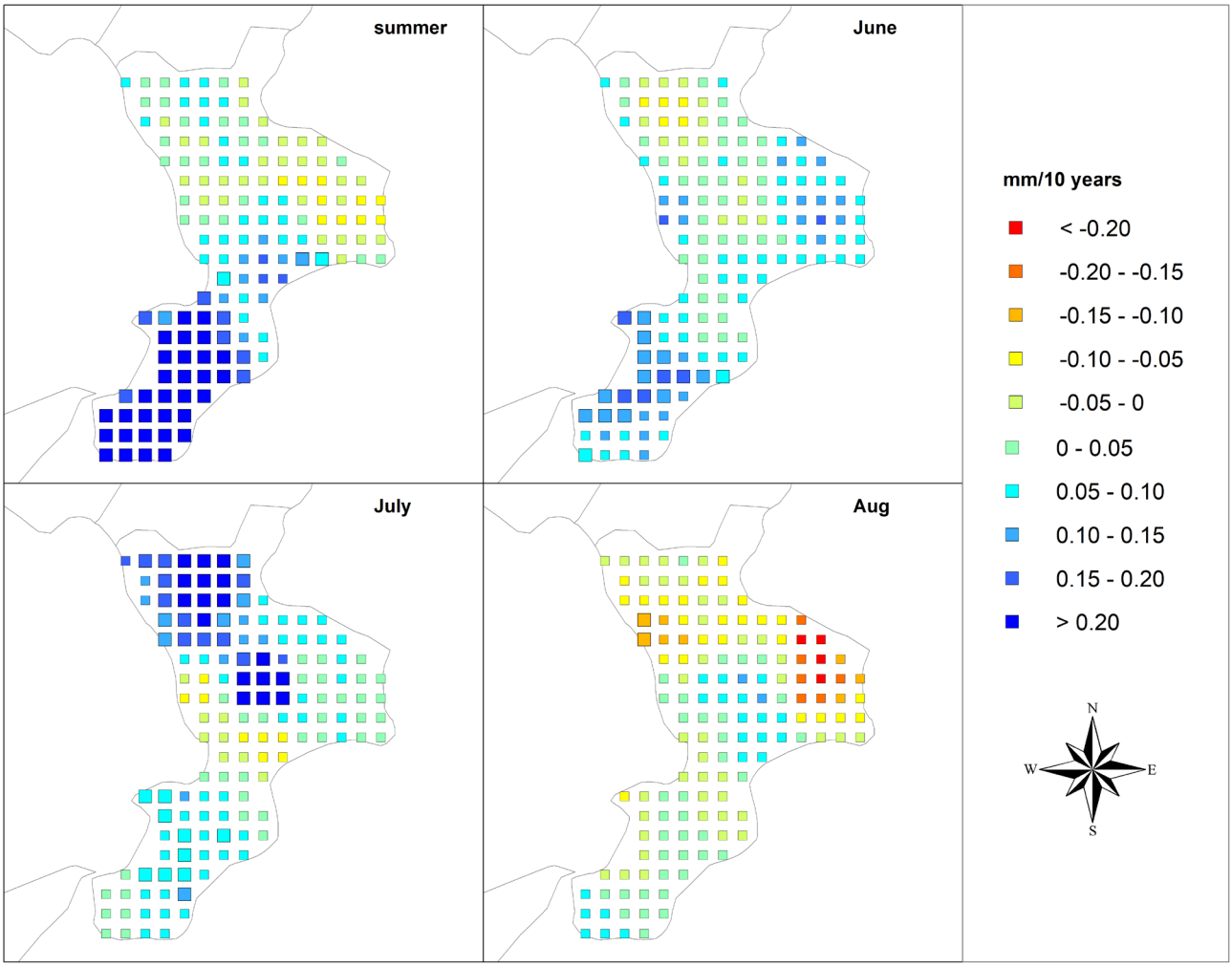

Figure 5. Spatial distribution of the trend results for summer obtained by means of the Theil–Sen estimator.

As a final consideration of the trend analysis, it can be stated that, besides the positive trend detected at annual scale, the tendencies are not uniform for all the seasons: positive in spring, summer and autumn, and negative for winter but with a few numbers of grid points involved (Figure 2). These not-uniform tendencies are also confirmed on a monthly scale. If September is the month with the highest number of grid points (about 62%) having positive tendencies, followed by April, July and March, months as January and October show negative tendencies. These results are also confirmed by the tendency on the temporal distribution of the occurrence of the yearly maximum 1-hr rainfall (Figure 7). In the first sub-period, the maximum values mostly occurred in October; in the more recent sub-period September is the month with the highest number of occurrences of the yearly maximum 1-hr rainfall.

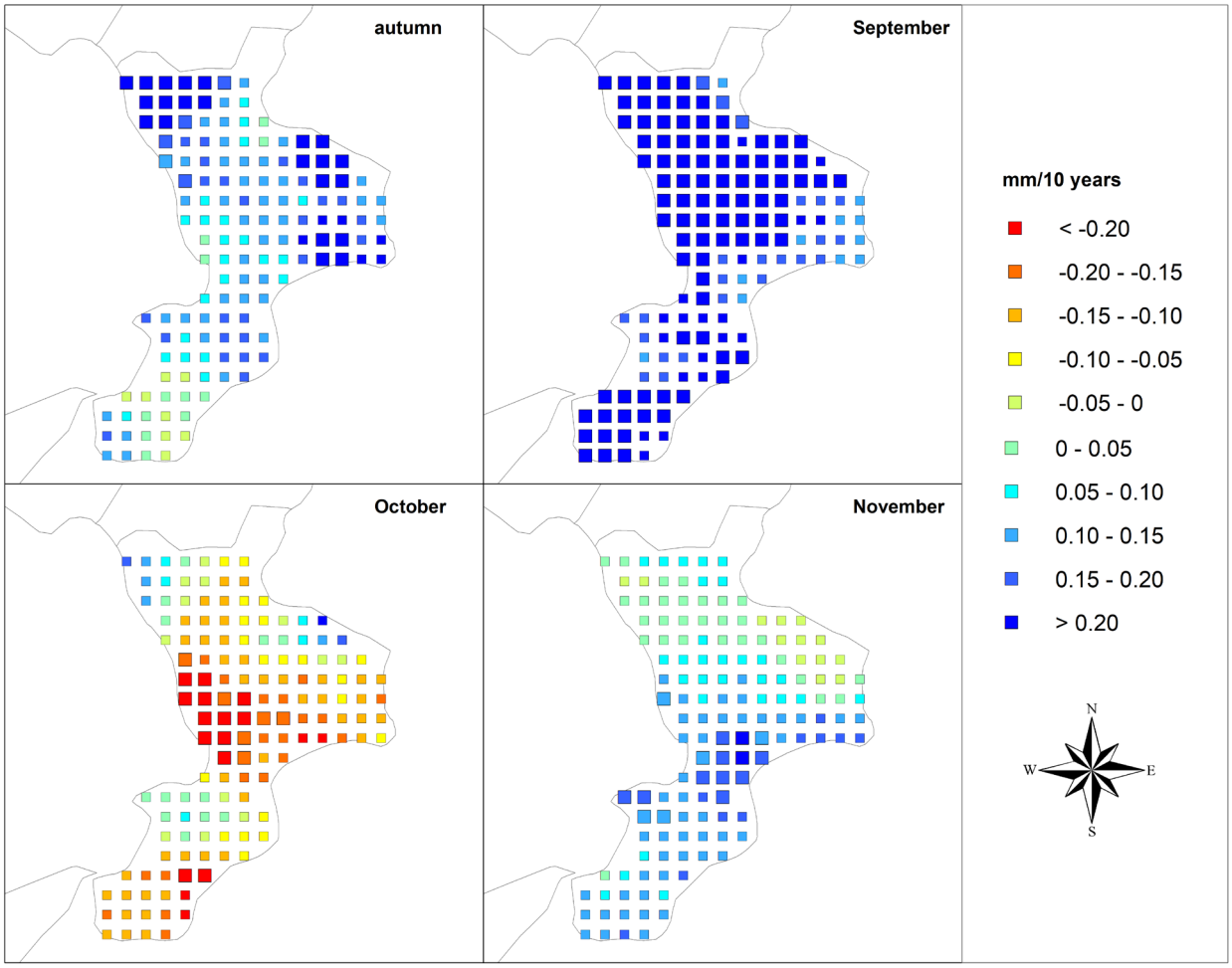

Figure 6. Spatial distribution of the trend results for autumn obtained by means of the Theil–Sen estimator.

Figure 7. Temporal distribution of the occurrences of the yearly maximum 1-hr rainfall in each sub-period.

5. CONCLUSIONS

The majority of Europe is expected to see an increase in the frequency of heavy precipitation events. Nevertheless, hourly precipitation records are frequently insufficient to examine trends and modifications in heavy rainfall. When direct measurements are not available, atmospheric reanalyses are a valuable source of long-term meteorological data. The ERA5 dataset (published by the ECMWF), used in this work for the Calabria region and regarding the 1-hour data, is one of the most advanced reanalyses currently accessible. On an annual basis, results indicated a positive

tendency for the maximum 1-hour rainfall. This tendency varies with the season; it is positive in the spring, summer, and fall and negative in the winter, but only involves a small number of cells. Monthly data also confirms these non-uniform tendencies. Concerning the temporal distribution of the annual maximum 1-hour rainfall, most of these values originally emerged in October. However, in the more recent 20-years sub-period out of the whole period 1961-2020, September has been the month with the most frequency of these values. This result is confirmed by recent damaging rainfall events that occurred in Calabria in the last weeks of the summer season, causing deaths and injuries too (e.g., Avolio et al. 2019). These trends should impose the land users to take a greater care of it, due to the strong impacts that these rainfall events can have on the territories.

REFERENCES

Ahammed, F., Alankarage Hewa, G., Argue, J.R., 2014. Variability of annual daily maximum rainfall of Dhaka, Bangladesh, Atmospheric Research; 137: 176-182.

Almendra-Martín, L., Martínez-Fernández, J., González-Zamora, Á., Benito-Verdugo, P., Herrero-Jiménez, C. M., 2021. Agricultural drought trends on the Iberian Peninsula: An analysis using modeled and reanalysis soil moisture products. Atmosphere; 12(2), 236.

Avolio, E., Cavalcanti, O., Furnari, L., Senatore, A., Mendicino, G., 2019. Brief communication: Preliminary hydro-meteorological analysis of the flash flood of 20 August 2018 in Raganello Gorge, southern Italy. Natural Hazards and Earth System Sciences; 19 (8): 1619–1627.

Bezak, N., Mikoš, M., 2020. Changes in the compound drought and extreme heat occurrence in the 1961–2018 period at the European scale. Water; 12(12), 3543.

Bharti, V., Singh, C., Ettema, J., Turkington, T. A. R., 2016. Spatiotemporal characteristics of extreme rainfall events over the Northwest Himalaya using satellite data: spatiotemporal characteristics of extreme rainfall events. Intern. Jour. Climatol.; 36: 3949–3962.

Caloiero, T., Coscarelli, R., Ferrari, E., 2020. Assessment of seasonal and annual rainfall trend in Calabria (southern Italy) with the ITA method. Journal of Hydroinformatics; 22.4.

Caloiero, T., Coscarelli, R., Gaudio, R., 2019. Spatial and temporal variability of daily precipitation concentration in the Sardinia region (Italy). Inter Jour Climatol; 39 (13): 5006-5021

Chen, S., Liu, B., Tan, X., Wu, Y., 2020. Inter-comparison of spatiotemporal features of precipitation extremes within six daily precipitation products. Climate Dynamics; 54: 1057–1076.

Colacino, M., Conte, M., Piervitali, E., 1997. Elementi di climatologia della Calabria. IFA-CNR, Rome, Italy.

Coscarelli, R., Caloiero, T., 2012. Analysis of daily and monthly rainfall concentration in Southern Italy (Calabria region). Journal of Hydrology; 416–417: 145-156.

Essou, G. R., Brissette, F., Lucas-Picher, P., 2017. The use of reanalyses and gridded observations as weather input data for a hydrological model: Comparison of performances of simulated river flows based on the density of weather stations. J. Hydrometeorol.; 18: 497-513.

Hanna, E., Cropper, T. E., Hall, R. J., Cornes, R. C., Barriendos, M., 2022. Extended North Atlantic Oscillation and Greenland blocking indices 1800–2020 from new meteorological reanalysis. Atmosphere; 13(3), 436.

Hersbach, H., Bell, B., Berrisford, P., et al. 2020. The ERA5 global reanalysis. Q J R Meteorol Soc.; 146: 1999–2049.

Hu, G., Franzke, C. L., 2020. Evaluation of daily precipitation extremes in reanalysis and gridded observation-based data sets over Germany. Geophys. Res. Lett.; 47(18), e2020GL089624.

Kendall, M.G., 1962. Rank Correlation Methods. Hafner Publishing Company, New York.

Kuo, Y.M., Chu, H.J., Pan, T.Y., Yu, H.L., 2011. Investigating common trends of annual maximum rainfalls during heavy rainfall events in southern Taiwan. Journal of Hydrol.; 409: 749–758.

Lagouvardos, K., Kotroni, V., Defer, E., Bousquet, O., 2013. Study of a heavy precipitation event over southern France, in the frame of HYMEX project: Observational analysis and model results using assimilation of lightning. Atmospheric Research; 134: 45-55.

Longo-Minnolo, G., Vanella, D., Consoli, S., Pappalardo, S., Ramírez-Cuesta, J. M., 2022. Assessing the use of ERA5-Land reanalysis and spatial interpolation methods for retrieving precipitation estimates at basin scale. Atmos. Res.; 271, 106131.

Mann, H.B., 1945. Nonparametric tests against trend. Econometrica; 13, 245–259.

Monteiro, D., Morin, S., 2023. Multi-decadal analysis of past winter temperature, precipitation and snow cover data in the European Alps from reanalyses, climate models and observational datasets. Cryosphere; 17: 3617-3660.

Muñoz Sabater, J., 2019. ERA5-Land hourly data from 1950 to present. Copernicus Climate Change Service (C3S) Climate Data Store (CDS). DOI: 10.24381/cds.e2161bac (Accessed on 10-May-2024)

Muñoz-Sabater, J., Dutra, E., Agustí-Panareda, A., Albergel, C., Arduini, G., Balsamo, G., Boussetta, S., Choulga, M., Harrigan, S., Hersbach, H., Martens, B., Miralles, D. G., Piles, M., Rodríguez-Fernández, N. J., Zsoter, E., Buontempo, C., Thépaut, J. N., 2021. ERA5-Land: A state-of-the-art global reanalysis dataset for land applications. Earth Syst. Sci. Data; 13: 4349-4383.

Palazzolo, N., Peres, D. J., Bonaccorso, B., Cancelliere, A., 2023. A Probabilistic Analysis of Drought Areal Extent Using SPEI-Based Severity-Area-Frequency Curves and Reanalysis Data. Water; 15(17), 3141.

Petroselli, A., Asgharinia, S., Sabzevari, T., Saghafian, B., 2020. Comparison of design peak flow estimation methods for ungauged basins in Iran. Hydrological Sciences Journal; 65 (1): 127–137.

Petroselli, A., De Luca , D.L., Młyński, D., Wałęga, A., 2022. Modelling annual maximum daily rainfall with the STORAGE (STOchastic RAinfall GEnerator) model. Hydrology Research; 53 (4): 547.

Reder, A., Raffa, M., Padulano, R., Rianna, G., Mercogliano, P., 2022. Characterizing extreme values of precipitation at very high resolution: An experiment over twenty European cities. Weather Clim. Extrem.; 35, 100407.

Sabzevari, T., 2017. Runoff prediction in ungauged catchments using the gamma dimensionless time-area method. Arabian Journal of Geosciences; 10 (6): 1–11.

Sen, P. K., 1968. Estimates of the regression coefficient based on Kendall's tau. Journal of the American Statistical Association; 63 (324): 1379–1389.

Siddique-E-Akbor, A. H. M., Hossain, F., Sikder, S., Shum, C. K., Tseng, S., Yi, Y., Turk, F. J., Limaye, A., 2014. Satellite precipitation datadriven hydrological modeling for water resources management in the Ganges, Brahmaputra, and Meghna Basins. Earth Interactions; 18: 1–25.

Sirangelo, B., Caloiero, T., Coscarelli, R., Ferrari, E., 2015. A stochastic model for the analysis of the temporal change of dry spells. Stoch. Environ. Res. Risk. Assess; 29:143–155.

Tabari, H., Talaee, P.H., 2011. Temporal variability of precipitation over Iran: 1966–2005. Journal of Hydrol.; 396 (3–4): 313–320.

Tarek, M., Brissette, F. P., Arsenault, R., 2020. Evaluation of the ERA5 reanalysis as a potential reference dataset for hydrological modelling over North America. Hydrol. Earth Syst. Sci.; 24: 2527-2544.

Turnipseed, D. P., Sauer, V. B., 2010. U.S. Geological Survey Techniques and Methods. A8; USGS, Ch. Discharge Measurements at Gaging Stations, 87.

Vicente-Serrano, S. M., Domínguez-Castro, F., Reig, F., Tomas-Burguera, M., Peña-Angulo, D., Latorre, B., Beguería, S., Rabanaque, I., Noguera, I., Lorenzo-Lacruz, J., El Kenawy, A., 2023. A global drought monitoring system and dataset based on ERA5 reanalysis: A focus on crop-growing regions. Geosci. Data J.; 10: 505-518.

Walega, A., Mlynnski, D., Bogdal, A., Kowalik, T., 2016. Analysis of the course and frequency of high water stages in selected catchments of the Upper Vistula Basin in the South of Poland. Water; 8(9): 394.

Wright, D. B., Smith, J. A., Villarini, G., Baeck, M. L., 2013. Estimating the frequency of extreme rainfall using weather radar and stochastic storm transposition. Journal of Hydrol.; 488: 150–165.

Xu, Z., Han, Y., Tam, C. Y., Yang, Z. L., Fu, C., 2021. Bias-corrected CMIP6 global dataset for dynamical downscaling of the historical and future climate (1979–2100). Sci. Data, 8(1), 293.